A Nonasymptotic Triple Deck Model for Supersonic Boundary-Layer Interaction

King-Mon Tu* and Sheldon Weinbaum†
The City College of The City University of New York, New York

This investigation presents an approximate nonasymptotic theory for the Lighthill-Stewartson triple-deck model of supersonic laminar boundary-layer interaction. The emphasis of the present study is on supersonic flows in the Reynolds number range $10^4 < Re < 10^6$, where the viscous sublayer is of comparable thickness to the inviscid interaction layer. The two principal simplifications of the lowest-order asymptotic theory, the neglect of the stream-tube divergence in the inviscid interaction layer, and compressibility effects in the sublayer, are examined in detail. Novel features of the theoretical development are the momentum integral treatment of the viscous sublayer and the separation pressure criterion used to determine its effective edge. Numerical solutions are presented for shock and wedge induced separation phenomena for Mach numbers in the range $2 \leq M_\infty \leq 10$. The theoretically predicted interaction pressure field is in good agreement with experimental measurement. One of the interesting new results is the gradual shift from the triple-deck to the single-layer description, since the Mach number increases as predicted by the recent asymptotic analysis of Brown, Stewartson, and Williams (see Ref. 7) for hypersonic interactions. The existence of supercritical-subcritical jumps observed in single-layer integral theories for highly cooled wall flows is also examined. Present results indicate that these jumps do not occur if the wall compatibility conditions derived from the boundary-layer equations are satisfied, and the integral averaging is performed across the sublayer alone.

Nomenclature

a = sonic velocity
c = constant Chapman viscosity law
h = static enthalpy
H = stagnation enthalpy
L = distance from the leading edge of the plate to start of interaction
M = Mach number
Pr = Prandtl number, $Pr = \mu C_p / K$
p = static pressure
Re = Reynolds number, $Re = \rho u x / \mu$
S = enthalpy function, $S = H/H_e - 1$
T = static temperature
u = longitudinal velocity component
U = transformed longitudinal velocity component, $U = \partial\psi/\partial Y$
v = normal velocity component
V = transformed normal velocity component, $V = -\partial\psi/\partial X$
x = longitudinal coordinate
X = transformed longitudinal coordinate, $dX = c(a_e/a_{0\infty})/(p_e/p_{0\infty})\,dx$
y = normal coordinate
Y = transformed normal coordinate, $dY = (a_e/a_{0\infty})(\rho/\rho_{0\infty})\,dy$
γ = ratio of specific heats
η = similarity variable, $\eta = (Y/X)\{[(m+1)/2](U_e X/\nu)\}^{1/2}$
μ = dynamic viscosity
ν = kinematic viscosity, $\nu = \mu/\rho$
ρ = mass density
τ = shear stress, $\tau = \mu(\partial u/\partial y)$
ψ = stream function
ϵ = sublayer thickness
E = transformed sublayer thickness
δ = boundary-layer thickness
Δ = transformed boundary-layer thickness
χ = interaction parameter
δ^* = transformed sublayer displacement thickness
θ^* = transformed sublayer momentum thickness

Subscripts

e = local flow outside the boundary layer
w = wall value
0 = stagnation value
∞ = freestream

Received Aug. 15, 1975; revision received Jan. 5, 1976. This work was supported by the Office of Naval Research under Navy Contract N00014-72-A-0406-0002. The authors wish to thank R. Melnik for many helpful comments.

Index category: Jets, Wakes, and Viscid-Inviscid Flow Interactions.

*Graduate Student, Department of Mechanical Engineering; present address: Mechanical Engineer, Center for Fire Research, Institute for Applied Technology, National Bureau of Standards, Washington, D.C. Associate Member AIAA.

†Professor, Department of Mechanical Engineering. Member AIAA.

I. Introduction

As first proposed by Lighthill[1] in his classic study of the upstream propagation of small disturbances in shock-wave boundary-layer interactions, the laminar boundary-layer equations for compressible flow in the limit of infinite Reynolds number exhibit a unique substructure if the pressure field driving the interaction is determined by the local flow inclination of the streamlines at the edge of the boundary layer. Asymptotic analysis of this substructure,[2-7] termed the triple-deck by Stewartson and Williams,[2,3] show that the streamwise length scale for supersonic self-induced separation interaction is of the order $Re^{1/8}\delta$, and that the boundary layer can be divided into two regions, a thin viscous sublayer ϵ of the order $Re^{-1/8}\delta$ and an inviscid interaction layer, which comprises the entire rest of the boundary layer, and thus is of the order δ.

The practical shortcoming of these supersonic asymptotic analyses is that, at the largest Re for which the boundary layer can be expected to remain laminar, $Re \approx 10^6$, the sublayer is at least $(1/5)\delta$, even for a highly cooled wall, and thus not a thin sublayer as required by the asymptotic theory. For hypersonic self-induced interactions, Neiland[5] has discovered a new asymptotic solution, valid in the limit $M_\infty{}^6 >> Re >> 1$, for which the thin sublayer structure vanishes and is replaced by a single viscous layer interaction originating at the leading edge of the plate. The recent analytic solutions of Brown, Stewartson, and Williams[7] for the limiting case $\gamma \to 1$ show that there is a smooth transition between the triple-deck and single-layer behavior as the parameter $\sigma \propto \chi^{1/4}/(\gamma-1)^{1/2}$ increases from zero to infinity, where $\chi = (M_\infty^3)/(Re^{1/2})$ is the hypersonic free-interaction parameter. Thus $\chi \to 0$ is the supersonic free in-

teraction limit and $\chi \to \infty$ is the hypersonic limit. The nondimensional scaling presented in the next section shows that σ or $\chi^{1/4}$ is, except for a multiplicative constant of order unity, proportional to ϵ/δ when $M_\infty >> 1$. The present numerical solutions for an adiabatic wall at $Re \approx 10^5$ to 10^6 show that ϵ increases from about 0.4 δ at $M_\infty = 2$ to about 0.7 δ at $M_\infty = 10$, and thus provides strong support for the smooth transition from the triple deck to the single-layer behavior predicted by the asymptotic analysis in Ref. 7. These results suggest that, for many high-speed laminar interaction problems of physical interest, $10^4 < Re < 10^6$, and $M_\infty < 10$ the substructure is still valid, but that the two simplifying features of the lowest-order asymptotic analysis that the sublayer can be treated as incompressible and that the stream tube divergence in the inviscid interaction layer can be neglected need to be examined more carefully.

It is not surprising, in view of the previous comments, that finite-difference[8-9] and integral approximation[10-13] single-layer theories provide better numerical agreement with experiment than the asymptotic analyses. The boundary-layer integral methods[10-13] have been extremely useful in providing approximate numerical solutions for nonadiabatic boundary-layer interaction phenomena. The application of the integral averaging technique employed in Refs. 10-12 introduces two important conceptual shortcomings. One is that the local velocity and enthalpy profiles are selected from the self-similar solutions of the compressible boundary-layer equations,[14,15] and thus are uncoupled from the local streamwise pressure gradient and the other compatibility conditions imposed by the boundary-layer conservation equations applied at the wall. The second shortcoming is the theoretically predicted existence of supercritical-subcritical jumps in highly cooled wall boundary-layer interactions. Sudden transitions of this type have not been observed experimentally.

In the framework of the original Crocco-Lees[16] theory, a supercritical boundary-layer cannot be triggered into a self-sustaining displacement interaction, and thus is stable with respect to downstream pressure disturbances. These boundary-layers first must undergo a supercritical-subcritical transition if they are to respond to a downstream compressive disturbance, such as shock wave or a compression corner. The theoretically predicted existence of sudden transitions of this type can not be satisfactorily resolved in the context of the single-layer integral theories or the lowest-order asymptotic analysis. There are two fundamental contributions to the outward displacement of inviscid streamlines at the outer edge of the boundary-layer. One is due to the viscous mass flow displacement of streamlines in the sublayer and is always positive (subcritical) for a compressive disturbance. The second contribution is due to the adiabatic expansion or contraction of stream-tube area in the inviscid interaction layer. This layer will behave subcritically or supercritically, depending upon whether the integral

$$\int_\epsilon^\delta \frac{M^2 - 1}{M^2} dy \gtrless 0 \tag{1}$$

discussed in Weinbaum and Garvine[17] is negative or positive, in that order. A boundary-layer with a subcritical inviscid interaction layer always will behave subcritically, whereas a boundary-layer with a supercritical inviscid interaction layer can hypothetically behave subcritically or supercritically, depending on whether the viscous sublayer or the inviscid interaction layer contributes more to the total stream-tube divergence of the entire boundary layer. Existing analyses are unable to answer this basic question, since the single-layer integral theories provide an inadequate description of the profiles near the wall, for the reasons discussed previously and the lowest-order asymptotic analyses neglect the stream-tube area changes in the inviscid interaction layer. The present triple-deck model for finite Reynolds numbers, by including both the proper wall compatibility conditions and compressibility effects in the sublayer and the stream-tube divergence in the inviscid layer, is able to explore in detail the relative importance of each layer to the overall pressure displacement interaction. The compressibility effects in the sublayer and the stream-tube divergence effects in the inviscid interaction layer, which are the focus of the present investigation, are the two principal first-order corrections in a series solution based on asymptotic matching techniques. The inclusion of these effects thus leads to a considerably better numerical agreement with experiment at finite *Re* than the lowest-order asymptotic solutions.

The mathematical treatment of each layer in the present nonasymptotic analysis of the Lighthill-Stewartson triple deck is as follows: the external flow is described by Prandtl-Meyer simple wave and oblique shock relations, the inviscid interaction layer is represented by a continuous distribution of rotational inviscid stream-tubes, and the viscous sublayer is approximated by a momentum integral of the conventional compressible boundary-layer equations, which takes into account the novel outer edge conditions for a viscous layer with nonvanishing edge gradients and the wall compatibility conditions for a nonadiabatic boundary-layer. A new family of fourth-order velocity profiles is introduced for the sublayer. This new profile family, since its description is confined only to a portion of the total boundary-layer, is capable of describing separated flow regions, provided that these regions are not of extended duration. In contrast, conventional quartic velocity profiles, which are used to describe the entire boundary-layer, are incapable of describing separated flow regions satisfactorily.[10] The present analysis thus is a significant advance beyond the earlier theory of Gadd,[18] which used a third-order velocity profile description for the sublayer, neglected the stream-tube divergence in the inviscid interaction layer, and therefore was capable of describing the flow interaction only up to separation. The asymptotic anslyses in Refs. 3,5, and 19 show that, for separated flows with a fully developed pressure plateau, the separated boundary-layer drives a separated flow region with an inviscid core, and the reattachment process is inviscid, as originally proposed by Chapman.[20] These flows with large separation regions lie outside the range of validity of the present theory.

Another unique feature of the present nonasymptotic analysis is the separation pressure criterion used to define the effective edge of the laminar sublayer. In the asymptotic analyses at infinite *Re*, the problem of locating ϵ does not arise, since the sublayer edge is defined only in an asymptotic sense.

II. Mathematical Formulation

A. Governing Equations and Coordinate Scaling

The fundamental equations governing the motion of a two-dimensional steady-state compressible viscous flow are the continuity and Navier-Stokes momentum and energy equations. Several authors[1,2,4,6,] have shown, by use of rational asymptotic ordering procedures, that in a region of supersonic free interaction the boundary-layer can be treated as two distinct layers, an inviscid interaction layer and an inner viscous sublayer, in which different sets of simpler approximate equations apply. An independent order-of-magnitude analysis of the various terms in the governing equations in each layer, as well as the scaling of all flow variables, is given by Tu in Ref. 21. Equivalent formulations are given in Refs. 2,6, and 8.

This dimensionless scaling shows that the characteristic streamwise distance for the separation induced interaction x_c, the sublayer thickness ϵ, and the ratio of sublayer to boundary-layer thickness ϵ/δ are given, respectively, by

$$\chi_c = L[(M_\infty^2 - 1)\, Re]^{-3/8} (Tw/T_\infty)^{3/2} \tag{2a}$$

$$\epsilon = 0[LRe^{-5/8} (M_\infty^2 - 1)^{-1/8} (Tw/T_\infty)^{3/2}] \tag{2b}$$

$$\epsilon/\delta = 0\{[(M_\infty^2 - 1)\, Re]^{-1/8} (Tw/T_\infty)^{1/2}\} \tag{2c}$$

For hypersonic adiabatic flows $T_w/T_\infty = 0(M_\infty^2)$, and Eq. (2c) reduces to $\epsilon/\delta = 0(M_\infty^{3/4}\, Re^{-1/8}) = 0(\chi^{1/4})$. The new parameter σ introduced in Ref. 7 is thus a measure of the ratio of sublayer to boundary-layer thickness. Equation (2c) suggests that the generalization of the hypersonic interaction parameter χ for supersonic free interactions is

$$\bar{\chi} = (M_\infty^2 - 1)^{-1/2}\, Re^{-1/2} M_\infty^4 \tag{2d}$$

One finds, by use of the dimensionless scaled coordinates based on Eqs. (2a) and (2b), that the sublayer equation of motion normal to the wall can be replaced to $0(\tilde{\chi}^{1/2})$ by $\partial P/\partial y = 0$. Thus, to this order, the governing equations for the sublayer are the conventional compressible boundary-layer equations

$$(\partial/\partial x)(\rho u) + (\partial/\partial y)(\rho v) = 0 \tag{3}$$

$$\rho u(\partial u/\partial x) + \rho v(\partial u/\partial y) = -dp/dx + (\partial/\partial y)[\mu(\partial u/\partial y)] \tag{4}$$

$$\rho u(\partial H/\partial x) + \rho v(\partial H/\partial y) = (\partial/\partial y)[\mu(\partial H/\partial y)] \tag{5}$$

where, in the boundary-layer energy equation [Eq. (5)], a Prandtl number of unity has been assumed. In the asymptotic theories,[2-4,6] where the sublayer is vanishingly thin, Eqs. 3-5 are replaced by their equivalent incompressible relations.

A similar ordering of the various terms in the inviscid interaction layer shows that the viscous terms in this layer are $0(\bar{\chi}^{1/2})$ less than the inertia and pressure terms and that the normal momentum equation again reduces to $0(\bar{\chi}^{1/2})$ to $\partial p/\partial y = 0$. The governing equations for the inviscid interaction layer thus simplify to $0(\bar{\chi}^{1/2})$ to the following:

$$(\partial/\partial x)(\rho u) + (\partial/\partial y)(\rho v) = 0 \tag{6}$$

$$\rho u(\partial u/\partial x) + \rho v(\partial u/\partial y) = -dp/dx \tag{7}$$

$$\rho u(\partial H/\partial x) + \rho v(\partial H/\partial y) = 0 \tag{8}$$

The boundary conditions which we shall impose on the sublayer velocity and stagnation enthalpy profiles require that these profiles match continuously in both value and slope with the profile descriptions in the inviscid interaction layer. Therefore, the matching conditions at $y = \epsilon$ are:

$$u = u_\epsilon \qquad \partial u/\partial u = (\partial_y/\partial y)_{\text{at } y=\epsilon} \qquad \psi = \psi_\epsilon$$
$$H = H_\epsilon \qquad \partial H/\partial y = (\partial H/\partial y)_{\text{at } y=\epsilon} \tag{9}$$

The sublayer edge condition used in the lowest-order asymptotic analyses[2-6] does not include either compressibility effects or the integrated stream-tube divergence in the inviscid interaction layer. The interaction pressure field applied at the sublayer edge thus is determined by the viscous displacement of the sublayer alone. The error introduced by this approximation is examined in Sec. III. The critical interaction equation relating the flow inclination at the sublayer and boundary-layer outer edge and the pressure in the inviscid external flow for the present analysis is derived in the next subsection.

At the wall, it is required that the sublayer velocity profile satisfy the no-slip condition and the two lowest-order wall compatibility conditions that obtain from the equation of motion, Eq. (4). Thus, at $y = 0$,

$$u = 0, \qquad (\partial/\partial y)[\mu(\partial u/\partial y)] = dp/dx$$
$$(\partial^2/\partial y^2)[\mu(\partial u/\partial y)] = 0 \tag{10}$$

Similarly, for the stagnation enthalpy profile, it is required that, at $y = 0$,

$$H = H_w, \qquad (\partial/\partial y)[\mu(\partial H/\partial y)] = 0 \tag{11}$$

The boundary conditions for Eqs. (6-8) for the inviscid interaction layer are the streamline inclination at the sublayer edge and the relationship between the pressure and the streamline inclination at the boundary-layer outer edge. The derivation of this basic formula for the interaction pressure field is presented next.

B. The Basic Interaction Relation

In accord with the foregoing remarks, the authors wish to derive an integrated stream-tube pressure-area relation for the inviscid interaction layer, which couples the viscous displacement effect at the edge of the sublayer to the interaction pressure imposed by the outgoing wave system at the edge of the boundary layer on the external flow. In order to accomplish this, one expresses the x derivatives of all flow variables in terms of dp/dx, using Eqs. (7) and (8), substitutes this result in Eq. (6), and then integrates the resulting expression across the free-interaction layer from ϵ to δ. This result

$$\tan\theta_e - \tan\theta_e = -\frac{1}{\gamma p}\frac{dp}{dx}\int_\epsilon^\delta \frac{M^2 - 1}{M^2}\, dy \tag{12}$$

couples the three flow regions. θ_e, the local flow angle at the boundary-layer edge, is determined by the local Mach number at the edge of the boundary layer through the use of the Prandtl-Meyer relation for the outer flow, which is assumed to be a simple outgoing wave system comprised of isentropic compression and expansion waves generated by the combined displacement interaction of the sublayer and free interaction layer. By use of the standard definition of the Prandtl-Meyer function $\nu(M)$,

$$\theta(x) = \nu(M_\infty) - \nu(M_e) - \theta_w(x) \tag{13}$$

where $\theta_w(x)$ is the inclination of the local wall tangent to the horizontal surface. θ_ϵ, the local streamline angle at the edge of sublayer, describes the displacement effect of the inner viscous region. The integral term on the right-hand side represents the integrated stream-tube/pressure-area relation for the free-interaction zone. This is an inviscid rotational flow with no normal pressure gradient, as discussed previously.

Since both the entropy s and the stagnation enthalpy H are conserved along each streamline in the inviscid interaction layer, one is led to the use of Von Mises coordinates x, ψ as the natural choice of coordinates for the inviscid interaction layer. Transforming Eq. (12) into Von Mises coordinates, one obtains

$$\tan\theta_e - \tan\theta_\epsilon = \frac{1}{\gamma p^2}\frac{dp}{dx}\frac{P_{0\infty}}{T_{0\infty}}\left(\frac{1}{\gamma R}\right)^{1/2} \times \int_{\psi_\epsilon}^{\psi_\delta} \frac{M^2(\psi,x) - 1}{M^3(\psi,x)}\, T^{1/2}(\psi,x)\, d\psi \tag{14}$$

The Mach number variation $M(\psi,x)$ along a streamline ψ is obtained directly from the isentropic pressure Mach number relation

$$M(\psi,x) = \left(\frac{2}{\gamma - 1}\right)^{1/2}\left\{\left(\frac{p_\infty}{p_1}\right)^{(\gamma-1)/\gamma} \times \left[1 + \frac{\psi - 1}{2} M_1^2(\psi)\right] - \right\}^{1/2} \tag{15}$$

where p_I and M_I (ψ) are known initial conditions at the start of the interaction, and $p(x)$ is the local pressure at the edge of the boundary-layer. Similarly, the temperature profile $T(\psi)$ is readily related to $M(\psi,x)$ given by Eq. (15) through the adiabatic streamline relation

$$T(\psi,x)=T_I(\psi)\frac{1+[(\gamma-1)/2]M_I^2(\psi)}{1+[(\gamma-1)/2]M^2(\psi,x)} \tag{16}$$

For a specified value of p_I and initial Mach number profile $M_I(\psi)$, it is evident from Eqs. (15) and (16) that the integral on the right-hand side of Eqs. (12) or (14) is only a function of the local interaction pressure $p(x)$ and the definitions ϵ and δ of the sublayer and boundary-layer edge. Equation (14) thus relates the integrated stream-tube divergence of the inviscid interaction layer $\theta_e-\theta_\epsilon$ to the local value of $p(x)$ and its gradient.

C. Treatment of the Viscous Sublayer

The solution of the boundary value problem for the sublayer is somewhat simplified if Eqs. (3-5) are first transformed to their incompressible form by introducing the modified Stewartson transformation employed by Cohen and Reshotko[14]

$$dX=c\frac{a_e}{a_{0\infty}}\frac{p_e}{p_{0\infty}}dx \quad dY=\frac{a_e}{a_{0\infty}}\frac{\rho}{\rho_{0\infty}}dy \tag{17}$$

$$U=\frac{a_{0\infty}}{a_e}u=\frac{\partial\psi}{\partial Y} \quad V=\frac{-\partial\psi}{\partial X} \quad S=\frac{H}{H_e}-1 \tag{18}$$

and a linear viscosity law assumed

$$\mu/\mu_{0\infty}=C(T/T_{0\infty}) \tag{19}$$

The momentum integral equation that one obtains after integrating the transformed equations across the sublayer and imposing the outer edge conditions (9) is

$$\frac{\partial\theta^*}{\partial X}-\frac{\theta^*}{U_E}\frac{dU_E}{dx}\left[2+\frac{\delta^*}{\theta^*}-\frac{E}{\theta^*}-\frac{U_e}{U_E}\times(dUe/dx)(dU_E/dx)\frac{1}{\theta^*}\int_0^E(1+S)dy\right]$$

$$-\frac{\nu_{0\infty}}{U_E^2}\frac{\tau_E}{\mu_E}+\frac{\nu_{0\infty}}{U_E^2}\frac{\tau_w}{\mu_w}=0 \tag{20}$$

where

$$\theta^*=\int_0^E\left(1-\frac{U}{U_E}\right)\frac{U}{U_E}dy \tag{21a}$$

$$\delta^*=\int_0^E\left(1-\frac{U}{U_E}\right)dy \tag{21b}$$

As one might anticipate, the new terms in the momentum integral equation [Eq.(20)] come from the nonvanishing shear stress τ_E at the sublayer edge $Y=E$ and the fact that conditions at $Y=E$ (the transformed sublayer edge) and $Y=\Delta$ (the transformed boundary-layer edge) differ. The transformed boundary conditions on the velocity and stagnation enthalpy profiles at the wall $Y=0$, obtained from Eqs. (10) and (11), are the same as those in conventional boundary-layer theory. They are expressed as follows:

$$U=0 \quad \frac{\partial^2U}{\partial Y^2}=\left(\frac{dp/dx}{\mu_{0\infty}(T_e/T_{0\infty})^{3/2}(p/p_{0\infty})\rho_w/\rho_{0\infty}}\right)$$

$$\frac{\partial^3U}{\partial Y^3}-\frac{1}{T_w}\frac{\partial T}{\partial Y}\frac{\partial^2U}{\partial Y^2}=0 \quad S=S_w \quad \frac{\partial^2S}{\partial Y^2}=0 \tag{22}$$

At $Y=E$, the transformed matching conditions (9) can be written

$$U=U_E \quad (\partial U/\partial Y)=(\partial U/\partial Y)_{\text{at } Y=E} \quad \psi=\psi_E$$

$$S=S_E \quad (\partial S/\partial Y)=(\partial S/\partial Y)_{\text{at } Y=E} \tag{23}$$

The selection of the sublayer velocity and stagnation enthalpy profiles to satisfy Eq. (20) and boundary conditions (22) and (23) is somewhat arbitrary. For present purposes, it was deemed sufficient to choose a fourth-order polynomial for the velocity and a third-order polynomial for the stagnation enthalpy. An improved description for nonadiabatic flows can be obtained by introducing a sublayer energy integral equation and a fourth-order polynomial for the stagnation enthalpy profile. The sublayer profiles used in the present study are summarized below; ξ is the dimensionless coordinate Y/E:

$$\frac{U}{U_E}=\frac{\xi}{3}(4-\xi^3)+\Lambda_1\frac{\xi}{6}\left[(2-3\xi+\xi^3)+\Lambda_4(1-3\xi^2+2\xi^3)\right]-\Lambda_2\frac{\xi}{3}(1-\xi^3) \tag{24}$$

$$\frac{S}{S_E}=\frac{\xi}{2}(3-\xi^2)+\frac{S_w}{S_E}\left(1-\frac{3}{2}\xi+\frac{\xi^3}{2}\right)-\Lambda_3\frac{\xi}{2}(1-\xi^2) \tag{25}$$

where the profile parameters Λ_i are defined by

$$\Lambda_1=\frac{dp/\mathrm{dx}}{\mu_{0\infty}(U_E/E^2)(T_e/T_{0\infty})^{3/2}/(p/p_{0\infty})(\rho_w/\rho_{0\infty})}$$

$$\Lambda_2=\frac{E}{U_E}\left(\frac{\partial U}{\partial Y}\right)_{\text{at } Y=E} \quad \Lambda_3=\frac{E}{S_E}\left(\frac{\partial S}{\partial Y}\right)_{\text{at } Y=E} \tag{26}$$

$$\Lambda_4=\frac{3(S_E-S_w)-S_E\Lambda_3}{6(1+S_w)}$$

Substituting the profile description [Eq. (24)] into Eq. (21), one can show readily that δ^* and θ^* are of the form

$$\theta^*=E(\alpha_1+\alpha_2\Lambda_1+\alpha_3\Lambda_1^2)$$

$$\delta^*=E(\alpha_4+\alpha_5\Lambda_1) \tag{27}$$

where the α_i are functions of Λ_2, Λ_3, and Λ_4. These three profile parameters depend on the sublayer edge conditions, and are evaluated at each station by calculating the normal velocity and temperature gradient at the lower edge of the inviscid interaction layer, using Eqs. (15) and (16).

D. Initial Conditions and Numerical Integration Procedure

It will be assumed that the flow upstream of the strong pressure interaction is that for a thin flat plate maintained at a constant temperature T_w, immersed at zero incidence in a uniform stream, whose Mach number is M_∞. The calculation of the flowfield in the interaction region is started at a distance x_1 from the leading edge, where the boundary-layer is assumed to be fully developed. The basic parameters that have to be specified for a typical interaction problem are M_∞, Re, and S_w. The velocity profile at position x_1 is determined by the standard Blasius solution, where distortions of the velocity profile due to interaction are small and can be neglected. At the initial station both p and dp/dx must be specified in order to start the pressure interaction.

The series expansion solution for a self-induced weak pressure interaction at high Mach number is given in Hayes and Probstein.[22] The weak interaction induced pressure for a flat plate with heat transfer is

$$p/p_\infty = 1.0 + d_{\text{orig}}\tilde{\chi} + [(\gamma+1)/4]\, d_{\text{orig}}{}^2\tilde{\chi}^2 \tag{28}$$

where

$$d_{\text{orig}} = \{1.0 + [(\gamma-1)/2]M_\infty^2\} \times (1.0+S_w)\ (0.865/M_\infty^2) + 0.166(\gamma-1)$$

and $\tilde{\chi}$ is the generalized interaction parameter defined by Eq. (2d). The initial value for dp/dx can be readily obtained by differentiating the preceding equation with respect to x.

The initial edge Mach number is obtained from

$$M_{e_1} = \left(\frac{2}{\gamma-1}\right)^{1/2}\left[\frac{1+[(\gamma-1)/2]M_\infty^2}{(P_1/P_\infty)^{(\gamma-1)/\gamma}}\right]^{1/2} \tag{29}$$

The initial temperature and enthalpy function profiles are given, respectively, by

$$T/T_e = (1+[(\gamma-1)/2]M_e{}^2)(1+S_w) - [(\gamma-1)/2]M_e{}^2(U/U_e)^2 \tag{30}$$

$$S = [1-(U/U_e)]S_w \tag{31}$$

In order to trigger the downstream pressure interaction, a small but finite pressure disturbance is imposed upon the weak interaction solution [Eq.(28)]. The basic unknown parameter in the numerical forward integration procedure is the location x_1 at which the interaction is initiated, as shown schematically in Fig. 1 for the case in which downstream compressive disturbance is an incident oblique shock wave. Changing the amplitude of the initial pressure perturbation is equivalent to adjusting the streamwise location at which the interaction is triggered, since all the solution curves shown in Fig. 1 are nearly the same up to separation. The small differences in these curves are due to the slight changes in the local values of Re at which the interaction is started.

The basic interaction equation [Eq.(14)] for the interaction pressure field is a second-order ordinary differential equation once θ_ϵ has been related to the sublayer profile descriptions. The uniqueness of the solution thus requires the specification of the initial pressure and location at which the interaction is triggered and the pressure downstream of the complete interaction. In the case of the shock-induced interaction sketched in Fig. 1, the latter pressure corresponds to the inviscid pressure in the external flow downstream of the single reflected shock that would occur if the boundary-layer were not present. As observed in Fig. 1, this downstream boundary condition determines the unknown location x_1 at which the interaction is initiated and the size of the separated flow region for a given strength incident oblique shock above the critical value for incipient separation. Lighthill[1] and Garvine[23] have demonstrated, by use of linearized models for the boundary-layer supersonic inviscid flow interaction, that the basic solution for the interaction pressure field contains two fundamental eigensolutions: one that decays to an undisturbed Blasius form, and a second that dies out exponentially upstream. Because of this second eigensolution, small departures from the weak interaction solution lead to large changes in downstream behavior. Thus, the split end-point boundary-value problem for the pressure is not best treated numerically, as an initial value problem. Numerical relaxation techniques, which take into account the downstream pressure boundary condition in the initial iteration, should be computationally more efficient in determining a unique solution than the trial-and-error forward integration procedure employed in the present study, which is described below. A relaxation technique of this type has been developed recently by Werle and Vatsa.[8]

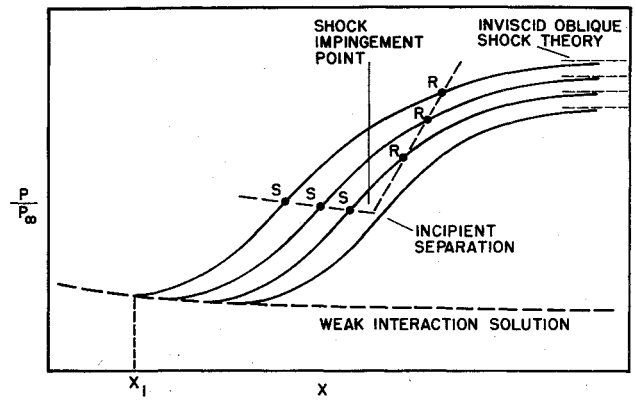

Fig.1 Schematic of shock-wave/boundary-layer interaction pressure curves.

The boundary-value problem for the present formulation of the triple deck requires that one obtain a simultaneous solution of Eqs. (14, 20, and 27), which satisfies the boundary condition (13), the matching conditions (23), and the initial conditions obtained from the weak interaction solution described previously. The numerical integration procedure that is adopted is based on the following forward difference approximations:

$$\delta_2 = \delta_1 + (\tan\theta_e)_1 \Delta x \tag{32a}$$

$$E_2 = E_1 + (\text{Tan}\theta_E)_1 \Delta x \tag{32b}$$

$$p_2 = p_1 + (dp/dx)_1 \Delta x \tag{32c}$$

$$\theta_2^* = \theta_1^* + (d\theta^*/dx)_1 \Delta x \tag{32d}$$

Here the subscripts 1 and 2 refer to streamwise locations x and $x+\Delta x$, respectively. At each station $\tan\theta_e$ is obtained from Eq. (13), $\tan\theta_\epsilon = \tan\theta_E$ from Eq. (14), $d\theta^*/dx$ from Eq. (20), and dp/dx from the definition of Λ_1, Eq. (26), and the solution of Eq. (27) for the new value of Λ_1. Since $\tan\theta_e$ is fixed by the pressure at the edge of the boundary-layer, Eq. (14) basically is a relation between $\tan\theta_E$ and the local pressure gradient dp/dx. The streamline ψ_ϵ, which serves as the effective sublayer edge, is determined by the separation pressure criterion described in the next subsection. The shape of this streamline is obtained from Eq. (32b).

In accord with the preceding comments, the forward integration proceeds as follows: The u, T, and M profiles at station 1 are assumed known, as well as S_w, S_E, δ_1, E_1 and θ_1^*. Λ_2, Λ_3, and Λ_4 at station 1 are evaluated on the basis of this known information, whereas Λ_1 is obtained from Eq. (27), using θ_1^*. The quadratic equation for Λ_1 has only one physically meaningful root, and this root is used to determine $(dp/dx)_1$. $(\tan\theta_E)_1$ now is found from Eq. (14). The finite-difference equations [Eq. (32)] now are applied to find the new values δ_2, E_2, p_2, and θ_2^*. The new u, T, and M profiles in the inviscid interaction layer are determined for the new pressure p_2 from Eqs. (15) and (16), and the new values of Λ_2, Λ_3, and Λ_4 are calculated. Equation (27) now is solved for the new value of Λ_1, and hence $(dp/dx)_2$. The new sublayer profiles are given by Eqs. (24) and (25), and $(\tan\theta_E)_2$ is calculated from Eq. (14). All of the flow parameters at station 2 now are known, and one can proceed to the next station, where the same procedure is repeated.

In the present study the initial location x_1 of the interaction is guessed, and the interaction is triggered by a small fixed amplitude perturbation from the weak interaction solution. Size of perturbation used was 0.1% above the weak interaction solution. Step sizes Δx for integration were $\Delta x =$

$\delta_1/200$ for $x \leq \delta_1$ and $x = \delta_1/50$ for $\Delta x > \delta_1$. The numerical results so obtained, when compared to the one using step size $\Delta x = \delta_1/500$, were within the accuracy of 2%.

E. Determination of the Sublayer Edge

The determination of the sublayer edge is somewhat subtle, since the transition from viscous to inviscid behavior in the interacting boundary-layer is gradual. Since one is attempting to predict the interaction pressure field, it is logical to choose a criterion for determining the sublayer edge which leads to a relatively invariant solution for this flow variable.

A unique feature of self-sustaining interactions due to compressive disturbances is that the pressure required to separate a specified boundary-layer profile is independent of the downstream disturbance. Both existing theories and experiments indicate that the incipient pressure at separation depends only upon M_∞, Re_∞, and S_w at the start of the interaction. Since the pressure at separation p_s in the present model depends on the definition of ϵ, one anticipates that, as the guessed value of the sublayer to boundary-layer thickness at the initial station ϵ_1/δ_1 is increased, one should eventually reach a value of ϵ_1/δ_1 where further increases should not produce significant changes in the predicted value of the incipient separation pressure as determined by a downstream integration, provided that an effective sublayer edge does exist. Furthermore, for this value of ϵ_1/δ_1 the predicted values of the interaction pressure field for the complete interaction should agree with experiment.

The numerical results for representative adiabatic and nonadiabatic boundary-layer profiles at various M_∞ are shown in Figs. 2-4. It is observed that for adiabatic boundary-layers the separation pressure becomes insensitive to ϵ_1/δ_1 and that a gradual maximum is achieved wherein further increase in ϵ_1/δ_1 only leads to a decrease in separation pressure because too much of the inviscid interaction flow is included in the viscous sublayer. The streamline ψ_ϵ at the effective edge of the sublayer has been chosen to correspond to this maximum in the separation pressure curves. The excellent agreement between theory and experiment throughout the entire pressure interaction for this choice of ψ_ϵ is evident from Fig. 5, where the solution has been continued through the points of separation and reattachment. In all of the calculations shown, the streamline at the edge of the sublayer ψ_ϵ has been held fixed. The value of ϵ/δ thus varies as the interaction proceeds. This procedure considerably simplifies the treatment of the inviscid interaction layer near the sublayer edge, since Eqs. (15) and (16) apply along a streamline.

Several general trends are discerned in Figs. 2-4. The sublayer in a highly cooled wall boundary-layer always is thinner and separates at a higher pressure than the adiabatic boundary-layer at the same Mach number. In both cases, the sublayer monotonically thickens as the Mach number and interaction parameter $\bar{\chi}$ increase. At $M_\infty = 10$, the largest value for the present study, $\bar{\chi} \approx 1.2$ and the sublayer has grown to about 0.7δ for the adiabatic case. The transition from the triple-deck to the single-layer structure, predicted by Brown, Stewartson and Williams,[7] is strongly suggested by these figures.

F. Flow Near Shock Impingement and Wedge Corner

The flow region in the immediate vicinity of shock impingement, lies outside the scope of the present analysis because of the important shock refraction effects that occur locally from the reflection of the incident shock wave. Experimental observations show that the viscous sublayer can not experience a sudden pressure rise. Thus, the reflection of the incident oblique shock at the sonic line is balanced by an equal strength but opposite reflected expansion fan.

In order to relate conditions across the region of shock impingement, we assume that on the length scale of the complete interaction this region can be viewed as a discontinuity in which the combined turning angle of the incident oblique shock wave and the reflected expansion fan are constant across the inviscid interaction layer. The velocity profile, enthalpy profile, and Mach number profile do not change on this length scale, and the static pressure is continuous. The

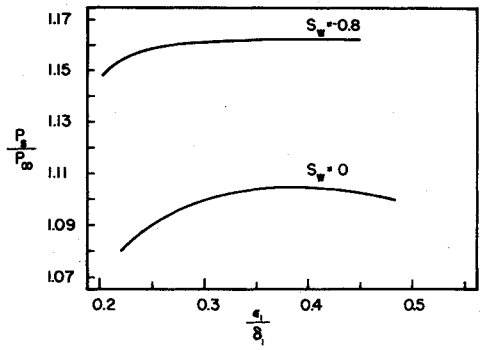

Fig.2 The dependence of the separation pressure on the sublayer edge for $M_\infty = 2$ and $Re_\infty = 1.85 \times 10^5$.

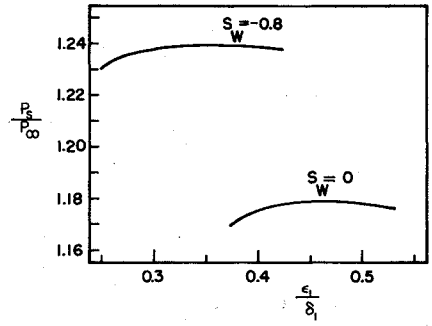

Fig.3 The dependence of the separation pressure on the sublayer edge for $M_\infty = 4.019$ and $Re_\infty = 10^6$.

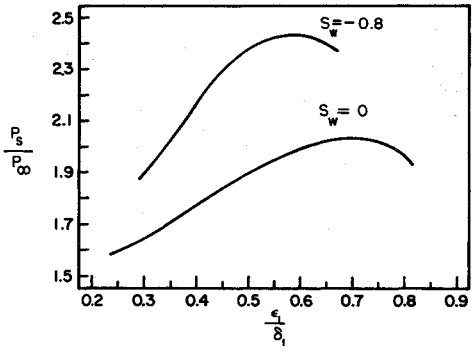

Fig.4 The dependence of the separation pressure on the sublayer edge for $M_\infty = 10$ and $Re_\infty = 0.73 \times 10^6$.

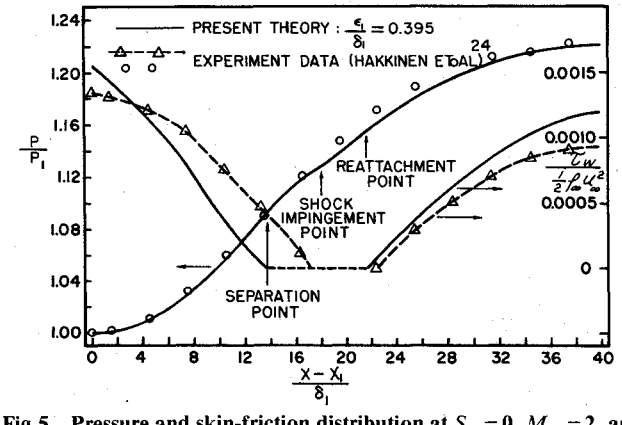

Fig.5 Pressure and skin-friction distribution at $S_w = 0$, $M_\infty = 2$, and $Re_\infty = 1.85 \times 10^5$.

streamline angles θ_e and θ_ϵ, however, are discontinuous because the flow streamlines at the boundary-layer and sublayer edge are turned by both the incident oblique shock and the reflected expansion fan. For a given shock strength, values of $\Delta\theta_e$ and $\Delta\theta_\epsilon$ are determined readily by use of the oblique shock and Prandtl-Meyer wave relations. The same mathematical model used to describe the interaction up to the location of shock impingement can be continued downstream. No difficulty is encountered in integrating Eqs. (14) and (20) through the reattachment point.

In the case of wedge-induced interaction the velocity profile, enthalpy profile and wall pressure are considered to be continuous at the wedge corner. However, the flow at the boundary-layer edge is deflected away from the wall through an angle equal to the wedge angle. For a given wedge angle, all conditions immediately downstream of the wedge corner are determined uniquely and the downstream integration can be performed without difficulty.

III. Numerical Results

A. Supercritical and Subcritical Behavior

As discussed in the introductory remarks, a supersonic boundary-layer can behave subcritically or supercritically, depending on whether the viscous displacement growth of the sublayer dominates the integrated stream-tube contraction of a supercritical inviscid interaction layer in the presence of a compressive downstream disturbance. The defining condition for a supercritical inviscid interaction layer, which was stated in Eq. (1), can be deduced directly from Eq. (12). One observes from Eq. (12) that the area of inviscid interaction layer will expand or contract, $(\theta_e - \theta_\epsilon) >$ or < 0, in an adverse pressure gradient, depending upon on the sign of the integral in Eq. (1).

Single-layer theories obviously are unable to describe the magnitude of the competing displacement effects in the sublayer and inviscid layer of the triple deck model. Furthermore, since the interaction problem is highly nonlinear, it does not follow that an integral average behavior for both layers, when lumped together, will be nearly the same as if they were treated individually, especially if velocity moments are taken in which the high-speed regions are weighted more heavily. Thus, it is not surprising that the results in Figs. 2-4 indicate an opposite behavior to that predicted by the integral average method of Klineberg and Lees[10] for the case of a highly cooled wall boundary layer with $S_w = -0.8$. The present results indicate that for this value of S_w the boundary layer is capable of a self-sustaining interaction leading to separation for all supersonic Mach numbers up to $M_\infty = 10$, the largest value of M_∞ examined. In addition, it is noteworthy that this subcritical behavior also was observed for values of ϵ_1/δ_1 which were obviously well within the viscous sublayer. The sudden supercritical-subcritical transitions predicted in the single-layer integral theories of Refs. 10 and 12 thus appear to be artifacts of the method, at least for the case $S_w = -0.8$, and are due to an inadequate treatment of the sublayer. Two possible causes of this difficulty are the omission of the wall compatibility conditions in the selection of the profiles, or an under-emphasis of the sublayer itself in an integral average technique where the averaging is performed across the entire boundary-layer.

In order to provide a more detailed insight into the competing viscous and inviscid displacement effects that are operative in a region of strong interaction, the authors plotted in Figs. 6 and 7 the stream-tube divergence or convergence between the inner and outer streamlines of the inviscid interaction layer up to the point of separation for both adiabatic and highly cooled boundary-layers. The three sets of curves given in Fig. 6 show how the streamline inclination at the edge of the sublayer and the edge of the boundary-layer change as the interaction proceeds toward separation for an adiabatic boundary-layer at several different Mach numbers. In all three cases, one observes that the viscous thickening of the

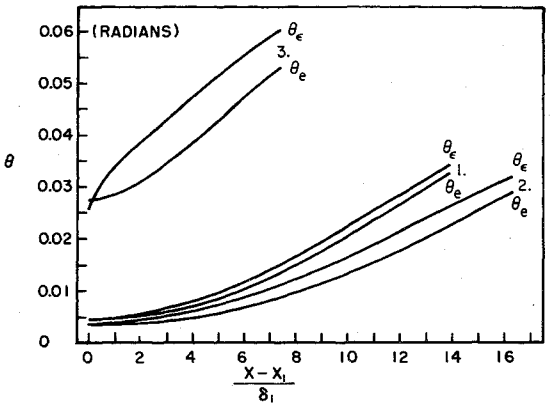

Fig.6 The stream-tube divergence or convergence between the inner and outer streamlines of the free interaction layer for adiabatic walls: 1. $S_w = 0$, $M_\infty = 2$, $Re_\infty = 1.85 \times 10^5$; 2. $S_w = 0$, $M_\infty = 4.019$, $Re_\infty = 10^6$; 3. $S_w = 0$, $M_\infty = 10$, $Re_\infty = 0.73 \times 10^6$.

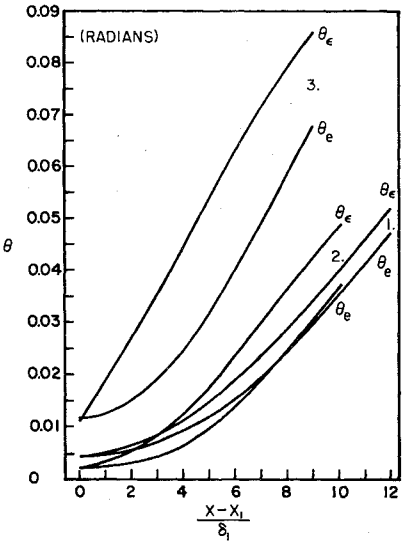

Fig.7 The stream-tube divergence or convergence between the inner and outer streamlines of the free interaction layer for nonadiabatic walls: 1) $S_w = -0.8$, $M_\infty = 2$, $Re_\infty = 1.85 \times 10^5$; 2. $S_w = -0.8$, $M_\infty = 4.019$, $Re_\infty = 10^6$; 3) $S_w = -0.8$, $M_\infty = 10$, $Re_\infty = 0.73 \times 10^6$.

sublayer more than compensates for the adiabatic contraction of the stream-tube area that occurs in the inviscid interaction layer. Although the sublayer edge moves outward as the Mach number increases (see Figs. 2-4), the stream-tube contraction in the inviscid interaction layer (the difference between θ_e and θ_ϵ) grows in importance as the Mach number increases. At $M_\infty = 2$, the stream-tube divergence in the inviscid interaction layer is negligible, whereas at $M_\infty = 4$ and 10, the inviscid adiabatic contraction of stream-tube area accounts for approximately 15 and 25% respectively, of the total streamline displacement interaction at separation. This effect again is not included in the lowest-order asymptotic theories of the triple-deck model.

Equivalent results for highly cooled nonadiabatic boundary-layer flows are shown in Fig. 7. These results show that the difference between θ_e and θ_ϵ is somewhat larger for a highly cooled laminar boundary-layer than for an adiabatic one at the same Mach number. This behavior is expected, since Figs. 2-4 show that wall cooling causes a larger fraction of the boundary-layer to behave inviscidly. One also observes that the dimensionless interaction distance to separation for a fixed amplitude initial perturbation is less than the corresponding adiabatic boundary-layer flow.

B. Shock-Wave Induced Interaction

A comparison of the present numerical solutions with the experimental measurements of Hakkinen et al.[24] for boun-

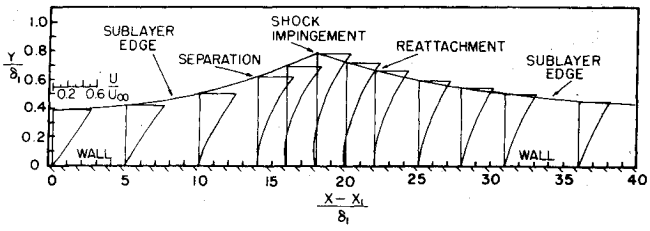

Fig.8 The sublayer velocity profiles at various positions for the $M_\infty = 2$ pressure interaction shown in Fig. 5.

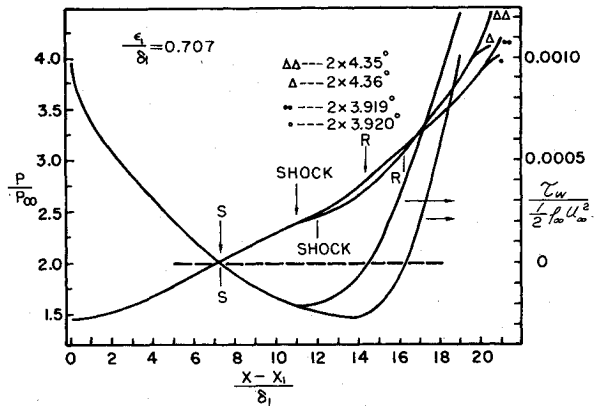

Fig.9 Pressure and skin-friction distribution at $S_w = 0$, $M_\infty = 10$, and $Re_\infty = 0.73 \times 10^6$.

dary-layer flow in a shock induced interaction at $M_\infty = 2$ and $Re_\infty = 1.85 \times 10^5$ is shown in Fig. 5. Pressure and wall skin-friction distributions obtained are in good agreement for the interaction region, both upstream and downstream of shock impingement. The flow across shock impingement point is discussed in Sec. II-F.

Figure 8 shows the sublayer velocity profiles at various positions for the $M_\infty = 2$ pressure interaction shown in Fig. 5. These profiles, with sublayer edge indicated, are plotted for the entire interaction through separation and reattachment. It is obvious that the sublayer velocity profiles are significantly deformed by the viscous effects.

Figure 9 shows the theoretically predicted pressure distribution for a representative adiabatic high Mach number flow at $M_\infty = 10$ and $Re_\infty = 7.3 \times 10^5$. The incident oblique shock wave has an inclination angle of approximately 2°. Theoretically, the relative position of the shock impingement point is determined by the downstream pressure in the inviscid outer flow, as discussed previously. In practice one finds that the numerical solutions downstream of shock impingement are very sensitive to the shock turning angle. Two types of downstream behavior are observed in Fig. 9, one characteristic of a second compressive disturbance further downstream and the second characteristic of a downstream expansion such as would occur at the base of the body. This behavior parallels the initial value behavior discussed in Ref. 23. Thus, having selected the point of shock impingement, the strength of the shock that allows the solution to proceed smoothly through reattachment is confined to a very narrow band of less than a tenth of a degree. The curves shown schematically in Fig. 1 represent the so-called "neutrally stable" solutions for the flow downstream of shock impingement. Larger increases in shock strength cause the shock impingement and reattachment points to move further downstream, and cause the length of the separation bubble to increase. Similar results have been obtained by previous investigators (see, for example, Klineberg and Lees [10]). The plot of the wall shear $\tau_w / \frac{1}{2}\rho_\infty U_\infty^2$ vs distance also is presented in Fig. 9.

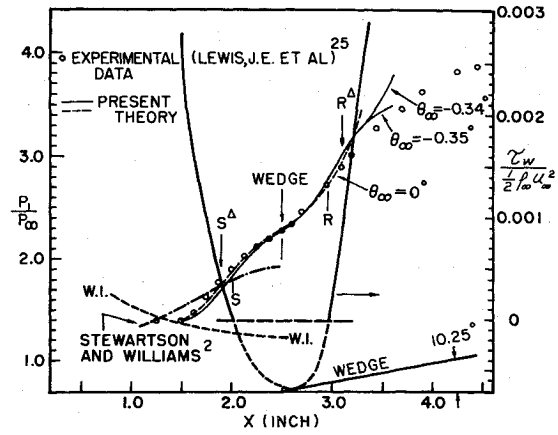

Fig.10 Pressure and skin-friction distribution at $S_w = 0$, $M_\infty = 6.06$, and $Re_\infty = 0.084 \times 10^6$; $\epsilon_1/\delta_1 = 0.715$.

C. Wedge-Induced Interaction

Figure 10 shows the comparison of the present theory with the experimental data obtained by Lewis et al. [25] for a wedge-induced adiabatic laminar boundary-layer interaction. The freestream Mach number is $M_\infty = 6.06$, and the freestream Reynolds number is $Re_\infty = 0.084 \times 10^6$. The wedge angle at the turning corner is 10.25 degrees.

The numerical solutions have been performed 1) with parallel flow conditions ($\theta_\infty = 0°$) and 2) with the assumption that the leading edge is at an angle of attack of $-0.34°$ ($\theta_\infty = -0.34°$) or $-0.35°$ ($\theta_\infty = -0.35°$). The theoretical pressure distribution curve, which provides the best agreement with the experimental measurements, is the case where the leading edge is at an angle of attack of $-0.35°$. The skin friction predicted by the theory is shown in the same figure. The general agreement shown between theory and experiment is extremely good, although the theoretically predicted separated flow region is somewhat shorter than the experimentally observed one.

According to Ko and Kubota, [26] the effect of the angle of attack is to change the static pressure measurement by a constant factor over the whole interaction zone, at least for the small angle range investigated. However, the present study shows that the numerical results far downstream of shock impingement point are very sensitive to the initial freestream flow direction at the starting point of interaction. Two types of downstream behavior are observed in Fig. 10, one characteristic of a second compressive disturbance further downstream and the second characteristic of a downstream expansive disturbance. This behavior parallels the initial value behavior just discussed in Fig. 9. A comparison with the asymptotic analysis by Stewartson and Williams [2] also is shown in Fig. 10. It is evident that the present theory provides numerical results that are significantly superior to the lowest-order asymptotic analysis for this case.

IV. Conclusions

An approximate nonasymptotic analysis has been formulated based on the three-layer conceptual model of Lighthill and Stewartson to describe the viscid-inviscid interaction in a laminar boundary-layer at finite Re_∞. The cornerstone of the analysis is the new interaction equation [Eq.(14)] relating the flow at the outer edge of the sublayer and the flow turning angle in the outer inviscid stream. With appropriate initial profiles specified and novel sublayer outer edge matching conditions satisfied, a continuous solution over the entire interaction field can be obtained by numerically integrating this interaction equation, together with an integral form of the governing equations for the sublayer. Numerical results have been obtained and compared with available experimental measurements for both shock-induced and wedge-induced viscid-inviscid interactions in

high-speed flights over adiabatic walls. Numerical calculations performed at Mach numbers of 2, 4.019, and 10, for both adiabatic and highly cooled flows, all indicate that viscid-inviscid laminar boundary-layer interactions are subcritical in nature.

The results presented in this study have been limited to displacement interactions involving relatively small separated flow regions whose dimensions are roughly of the same order as the interaction distance to separation. For stronger compressive disturbances, the present family of fourth-order sublayer velocity profiles must be modified if one is to obtain a pressure plateau characteristic of extended separated flow regions. The basic difficulty can be surmised from the asymptotic analysis of Stewartson and Williams,[3] who show that the separated flow region has an inviscid core with a separated free shear layer at its upper boundary, and a reverse flow boundary-layer near the wall.

References

[1] Lighthill, M.J., "On Boundary-Layers and Upstream Influence, II. Supersonic Flows without Separation," A,217, 1953; pp. 478-507.

[2] Stewartson, K., and Williams, P.G. "Self-Induced Separation," Proceedings of the Royal Society (London), Vol. A312, 1969, pp. 181-206.

[3] Stewartson, K, and Williams, P.G., "On Self-Induced Separation II," *Mathematika,* Vol. 20, 1973, pp. 98-108.

[4] Messiter, A.F., Hough, G.R., and Feo, A., "Base Pressure in Laminar Supersonic Flow," *Journal of Fluid Mechanics,* Vol. 60, Pt. 3, 1973, pp. 605-624.

[5] Neiland, V.Y., *Izy, Alademiia Nauk* SSSR Meh. Aidk. 1971, pp. 19-24.

[6] Jenson, R., Burggraf, O., and Rizzetta, D., *Proceedings 4th of the International Conference on Numerical Methods in Fluid Mechanics,* Springer-Verlag, 1974.

[7] Brown, S.N., Stewartson, K., and Williams, P.G., "Hypersonic Self-Induced Separations," *Physics of Fluids,* Vol. 18, June 1975, pp. 633-639.

[8] Werle, M.J. and Vatsa, V.N., "New Method for Supersonic Boundary-Layer Separations," *AIAA Journal,* Vol. 12, Nov. 1974, pp. 1491-1497.

[9] Reyhner, T.A. and Flugge-Lotz, I., "The Interaction of a Shock Wave with a Laminar Boundary-Layer," *International Journal of Non-Linear Mechanics,* Vol. 3, Pergamon Press, New York, 1968, pp. 173-199.

[10] Klineberg, J.M. and Lees L., "Theory of Laminar Viscid-Inviscid Interactions in Supersonic Flow," *AIAA Journal* Vol. 7, Dec. 1969, pp. 2211-2221.

[11] Holden, M.S., "Theoretical and Experimental Studies of Laminar Flow Separation on Flat Plate Wedge Compression Surfaces in the Hypersonic Strong Interaction Regime," Cal. Rept. AF-1894-A-2, May 1967.

[12] Georgeff, M.P., "Momentum Integral Method for Viscous-Inviscid Interactions with Arbitrary Wall Cooling," *AIAA Journal,* Vol. 12, Oct. 1974, pp. 1393-1400.

[13] Nielsen, J.N., Lynes, L.L., and Goodwin, F.K., "Calculation of Laminar Separation with Free Interaction by the Method of Integral Relations, Part I – Two Dimensional Supersonic Adiabatic Flow, Oct. 1965. Part II – Two Dimensional Supersonic Non-Adiabatic Flow and Axisymmetric Supersonic Adiabatic and Non-Adiabatic Flows," AFFDL TR 65-107, Jan. 1966, Air Force Flight Dynamics Laboratory, Wright-Patterson Air Force Base, Ohio.

[14] Cohen, C.B. and Reshotko, E., "Similar Solutions for the Compressible Laminar Boundary-Layer with Heat Transfer and Pressure Gradient," NASA Rept. 1293, 1956.

[15] Stewartson, K., "Further Solutions of the Falkner-Skan Equation," *Proceedings of the Comb. Philosophical Society* Vol. 50, 1954, pp. 454-465.

[16] Crocco, L. and Lees, L., "A Mixing Theory for the Interaction between Dissipative Flows and Nearly Isentropic Streams," *Journal of the Aeronautical Sciences,* Vol. 19, Oct. 1952, pp. 649-676.

[17] Weinbaum, S. and Garvine, R.W., "On the Two Dimensional Viscous Counterpart of the One Dimensional Sonic Throat," *Journal of Fluid Mechantics,* Vol. 39, Pt. 1, 1969, pp. 57-85.

[18] Gadd, G.E., "A Theoretical Investigation of Laminar Separation in Supersonic Flow," *Journal of the Aeronautical Sciences,* Vol. 24, Oct. 1957, pp.759-772.

[19] Burggraf, O.R., "Asymptotic Theory of Separation and Reattachment of a Laminar Boundary-Layer on a Compression Ramp," *Proceedings of the AGARD Symposium on Flow Separation,* Gottingen, Germany, May 27-30, 1975.

[20] Chapman, D.R., NACA TN 3792, 1956.

[21] Tu, King-Mon, "Viscid-Inviscid Flow Interactions," Ph.D. thesis, The City University of New York, 1975.

[22] Hayes, W.D. and Probstein, R.F., *Hypersonic Flow Theory,* 2nd ed., Vol. I. Academic Press, New York, 1966.

[23] Garvine, R.W., "Upstream Influence in Viscous Interaction Problems," *Physics of Fluids,* Vol. 11, 1968, pp. 1413-1423.

[24] Hakkinen, R.J., Greber, I., Trilling, L., and Abarbanel, S.S., "The Interaction of an Oblique Shock Wave with a Laminar Boundary-Layer," NASA Memo. 2-18-59, March 1959.

[25] Lewis, J., Kubota, T., and Lees, L., "Experimental Investigation of Supersonic Laminar, Two Dimensional Boundary-Layer Separation in a Compressional Corner with and without Cooling," *AIAA Journal,* Vol. 6, Jan. 1968, pp. 7-14.

[26] Ko, D.R.S. and Kubota, T., "Supersonic Laminar Boundary-Layer along a Two Dimensional Adiabatic Curved Ramp," *AIAA Journal,* Vol. 7, Feb. 1969, pp. 298-304.